

A BIJECTION BETWEEN PATHS FOR THE $\mathcal{M}(p, 2p+1)$ MINIMAL MODEL VIRASORO CHARACTERS

OLIVIER BLONDEAU-FOURNIER, PIERRE MATHIEU, AND TREVOR WELSH

ABSTRACT. The states in the irreducible modules of the minimal models can be represented by infinite lattice paths arising from consideration of the corresponding RSOS statistical models. For the $\mathcal{M}(p, 2p+1)$ models, a completely different path representation has been found recently, this one on a half-integer lattice; it has no known underlying statistical-model interpretation. The correctness of this alternative representation has not yet been demonstrated, even at the level of the generating functions, since the resulting fermionic characters differ from the known ones. This gap is filled here, with the presentation of two versions of a bijection between the two path representations of the $\mathcal{M}(p, 2p+1)$ states.

In addition, a half-lattice path representation for the $\mathcal{M}(p+1, 2p+1)$ models is stated, and other generalisations suggested.

1. INTRODUCTION

The corner-transfer matrix is a powerful tool for expressing the local state probabilities of the order variable in terms of weighted sums of one-dimensional configurations [2]. For the restricted-solid-on-solid (RSOS) models [1, 11] in regime III (in the infinite length limit), each weighted configuration sum turns out to be the character of an irreducible module of the corresponding minimal model [5, 19]. Each configuration is the specification of the order variable's value at each position, with fixed extremities, and the differences between neighbouring values constrained. When dressed with edges linking adjacent points, it becomes a lattice path. Every state in the corresponding conformal theory is thus represented by a particular lattice path [21, 7].

This path description of the states has proved to be a royal road for the construction of the fermionic characters [17], either using direct methods [21, 16], or recursive ones [7, 10, 23]. For the special class of minimal models $\mathcal{M}(p, 2p+1)$, an alternative path representation was found in [15], and this led to novel fermionic expressions. These paths, however, were not deduced from a statistical model whose scaling limit was known to be the $\mathcal{M}(p, 2p+1)$ minimal model. Moreover, their generating functions have not, hitherto, been proved to be equivalent to either the bosonic expressions [20] or the usual fermionic expressions [17, 8, 10, 23, 16] for these characters (although the equivalence has been checked to high order, and was supported by an asymptotic analysis). Albeit formally ad hoc, the discovery of this new path representation relied on heuristic considerations which we briefly recall.

Like their scaling limit, the RSOS models are parameterised by two relatively prime positive integers p, p' with $p' > p \geq 2$.¹ The corresponding paths are sequences of NE and SE edges restricted to the interior of an infinite strip of vertical width $p' - 2$ (this definition is made more precise in Section 2.2). The weight of each path is the sum of the weights

May 11, 2018.

¹For the RSOS models/paths, we follow the notation used in [11, 7, 23, 10]. Consequently, the corresponding notation for the minimal models differs from that of [6, 16] by the interchange of p and p' . This interchange is of course irrelevant, the physical characteristics, the conformal dimensions

$$h_{r,s} = \frac{[r \max(p, p') - s \min(p, p')]^2 - (p - p')^2}{4pp'}$$

of the highest-weight states in modules labelled by (r, s) for $1 \leq r < \min(p, p')$ and $1 \leq s < \max(p, p')$, remain unchanged.

of its vertices. The weight of a vertex depends not only upon its shape, but also upon the two parameters p and p' [11]. In the unitary cases (those cases where $p' = p + 1$), a drastic simplification occurs in that the peaks and the valleys of a path do not contribute to its weight, while every other vertex contributes $x/2$, where x is its horizontal position. On the other hand, weighting the path in the dual way (assigning weight $x/2$ to the valleys and peaks and 0 to all other vertices) leads to the character of the \mathcal{Z}_{p-1} parafermionic models [3, 21, 5, 9]. These cases were then contrasted with the paths describing the states of the graded versions of these parafermionic models – equivalent to the cosets $\widehat{osp}(1, 2)_{p-1}/\widehat{u}(1)$ [4, 12]. These latter paths reside on a half-integer lattice with only peaks and valleys contributing to the weight, each to the amount $x/2$, and with the special constraint that peaks are forced to occur at integer heights.² Seeking their dual versions led to the new path description of the $\mathcal{M}(p, 2p + 1)$ models [15].

The demonstration of the correctness of this new path description of the $\mathcal{M}(p, 2p + 1)$ states is the main subject of the present work. This is achieved by exhibiting a bijection between these paths and the RSOS paths. In fact, two equivalent but quite different-looking versions of this bijection are presented.

After defining the two types of path in Section 2, the first version of the bijection is presented in Section 3. It relies on techniques developed in [7, 23]. It essentially amounts to the deconstruction of an RSOS path, followed by a corresponding construction of a half-lattice path. The second version of the bijection is presented in Section 4. It relies on an encoding of the vertex words for RSOS paths introduced in [22], and an analogous construction for the half-lattice paths that is a modification of that given in [14]. In this approach, each path, with given extremity conditions, is constructed from a sequence of operators acting on a suitable ground-state path. The bijection is expressed as a rule for transforming between sequences of operators that describe the two paths. Although the two versions of the bijection were originally obtained independently, we show in Section 4.3 that the second is, in fact, a transformation of the first, thereby immediately obtaining its proof.

2. DEFINING THE TWO TYPES OF PATHS

2.1. α -Lattice paths. An infinite length α -lattice path h is a sequence $(h_0, h_\alpha, h_{2\alpha}, \dots)$ for which $|h_{x+\alpha} - h_x| = \alpha$ for $x \in \alpha\mathbb{Z}_{\geq 0}$. The path h is said to be (f, g) -restricted if $f \leq h_x \leq g$ for all $x \geq 0$ and b -tailed if there exists $L \geq 0$ such that $h_x \in \{b, b - \alpha\}$ for all $x \geq L$. In this work, we consider two cases: $\alpha = 1$ (integer lattice paths) and $\alpha = 1/2$ (half-lattice paths).

By linking the points $(0, h_0), (\alpha, h_\alpha), (2\alpha, h_{2\alpha}), \dots$ on the x - y plane we obtain a graph that conveniently depicts the path: we refer to this graph as the path picture. For each $x > 0$, the position (x, h_x) on the path picture of h is referred to as a vertex. The shape of the vertex is either a peak, valley, straight-up or straight-down depending on whether the edges on the two sides of the vertex are NE-SE, SE-NE, NE-NE or SE-SE, respectively.

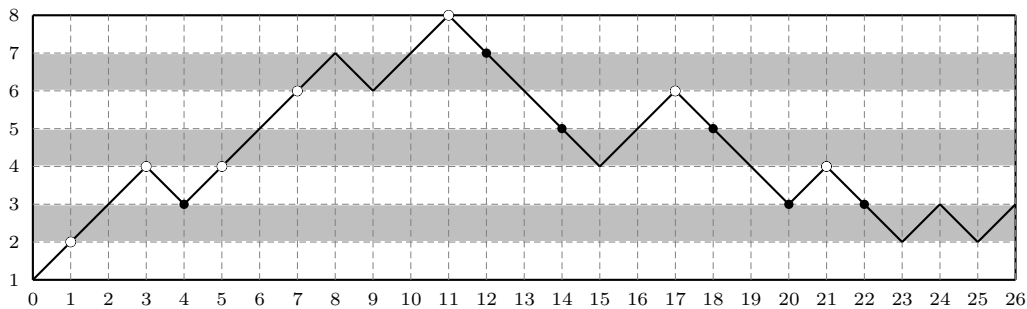
On occasion, it will be necessary to refer also to the position $(0, h_0)$ as a vertex, and to have its shape determined. When required, this is done by specifying the value of $h_{-\alpha}$ to be one of the two values $h_0 \pm \alpha$. In effect, this defines the direction of a path pre-segment.

²The usual parafermionic states have two path representations, bijectively related in [13] (see also [18] and references therein). This is also true for the graded ones [15, §5]. We are referring here to the RSOS-type path representation (with no horizontal edges).

2.2. RSOS paths and the $\mathcal{M}(p, p')$ models. The set $\mathcal{P}_{a,b}^{p,p'}$ of RSOS paths is defined to be the set of infinite³ length integer lattice paths h that are $(1, p' - 1)$ -restricted, b -tailed, with $h_0 = a$. Each RSOS path $h \in \mathcal{P}_{a,b}^{p,p'}$ is assigned a weight $wt(h)$ which we now define.⁴

For $1 \leq k \leq p' - 1$, we refer to the region of the x - y plane between $y = k$ and $y = k + 1$ as the k th band. Thus, in the path picture, the paths from $\mathcal{P}_{a,b}^{p,p'}$ lie in the $p' - 2$ bands between $y = 1$ and $y = p' - 1$. For $1 \leq r < p$, we shade the $\lfloor rp'/p \rfloor$ th band and refer to it as the r th dark band. Bands that are not dark are referred to as light bands.⁵ The band structure for the case $(p, p') = (4, 9)$, along with a typical path from $\mathcal{P}_{1,3}^{4,9}$, is shown in Fig. 1. This band pattern is typical of all models with $p' = 2p + 1$: there are $p - 1$ dark bands separated from each other by a single light one.

Figure 1: A path $h \in \mathcal{P}_{1,3}^{4,9}$. The unfilled circles indicate up-scoring vertices, which have weight u_x , and the filled circles indicate down-scoring vertices, which have weight v_x , both values being defined in (1).



Those vertices which either are straight with the right edge in a dark band, or are not straight with the right edge in a light band, are referred to as *scoring* vertices. All other vertices are referred to as *non-scoring* vertices. Each scoring vertex is said to be *up-scoring* or *down-scoring* depending on whether the left edge is up or down respectively. In the path picture, we (often) highlight the up-scoring vertices with an unfilled circle, and the down-scoring vertices with a filled circle. This is done for the path of Fig. 1.

After setting⁶

$$(1) \quad u_x = \frac{1}{2}(x - h_x + a) \quad v_x = \frac{1}{2}(x + h_x - a),$$

the weight $wt(h)$ of a path h is defined to be:

$$(2) \quad wt(h) = \sum_{x>0} w_x,$$

³These paths were originally defined for finite length in [11] and studied extensively in [7, 10, 23]. The collection of finite paths (with specific boundary conditions) provides a finitized version of the Virasoro characters [19]. The finitization parameter enables the derivation of useful recurrence relations for the path generating functions. In particular, one can define the notion of dual finitized characters, which are obtained via the transformation $q \rightarrow 1/q$ [3, 21, 7, 15].

⁴The definition given here is that of [7]. It differs considerably from that originally given in [11]. In fact, although this is not obvious, the weighting of the paths $\mathcal{P}_{a,b}^{p,p'}$ defined in [11] differs from that of [7] by an overall constant depending upon a and b .

⁵In [7, 10, 23], dark and light bands were referred to as odd and even bands respectively.

⁶The point (x, h_x) has coordinates (u_x, v_x) in the system where the axes are inclined at 45° , and the origin is at the path startpoint.

where we define

$$(3) \quad w_x = \begin{cases} u_x & \text{if } (x, h_x) \text{ is up-scoring;} \\ v_x & \text{if } (x, h_x) \text{ is down-scoring;} \\ 0 & \text{if } (x, h_x) \text{ is non-scoring.} \end{cases}$$

For the path h depicted in Fig. 1, we obtain

$$(4) \quad wt(h) = 0 + 0 + 3 + 1 + 1 + 2 + 9 + 9 + 6 + 11 + 11 + 9 + 12 = 74.$$

The tail condition of an RSOS path h indicates that after a certain position, the path forever oscillates within a single band. The definition (2) then implies that $wt(h)$ is finite or infinite depending on whether this band is dark or light respectively. Below, we restrict to those cases where that band is dark.

The paths in the set $\mathcal{P}_{a,b}^{p,p'}$ provide a combinatorial description of the states in the irreducible module of the minimal model $\mathcal{M}(p, p')$ that is labelled by (r, s) , where the extremity points a and b are related to r and s by

$$(5) \quad a = s \quad \text{and} \quad b = \lfloor rp'/p \rfloor + 1.$$

(Thereupon, the heights b and $b - 1$ straddle the r th dark band of the path picture). The generating function of the set $\mathcal{P}_{a,b}^{p,p'}$ of paths is then the Virasoro character $\chi_{r,s}^{p,p'}$ [7]:

$$(6) \quad \sum_{h \in \mathcal{P}_{a,b}^{p,p'}} q^{wt(h)} = \chi_{r,s}^{p,p'}(q).$$

2.3. $\mathcal{M}(p, 2p + 1)$ characters and half-lattice paths. The states in the irreducible modules of the $\mathcal{M}(p, 2p + 1)$ models turn out to have a path representation alternative to that specified above. This description was first given in [15].

For $p \geq 2$ and $\hat{a}, \hat{b} \in \mathbb{Z}$, define $\mathcal{H}_{\hat{a}, \hat{b}}^p$ to be the set of all half-lattice paths \hat{h} that are $(0, p-1)$ -restricted, \hat{b} -tailed, with $\hat{h}_0 = \hat{a}$, and the *additional* restriction that if $\hat{h}_x = \hat{h}_{x+1} \in \mathbb{Z}$, then $\hat{h}_{x+1/2} = \hat{h}_x - 1/2$. The additional restriction here implies that peaks can only occur at integer heights.

For each path $\hat{h} \in \mathcal{H}_{\hat{a}, \hat{b}}^p$, we specify the shape of the vertex at its startpoint $(0, \hat{a})$ by adopting the convention that $\hat{h}_{-1/2} = \hat{a} - 1/2$ (we do this even if $\hat{a} = 0$).

The *unnormalised* weight $\hat{w}^\circ(\hat{h})$ of a path $\hat{h} \in \mathcal{H}_{\hat{a}, \hat{b}}^p$ is defined to be half the sum of those $x \in \frac{1}{2}\mathbb{Z}_{\geq 0}$ for which (x, \hat{h}_x) is a straight-vertex:

$$(7) \quad \hat{w}^\circ(\hat{h}) = \frac{1}{2} \sum_{\substack{x \in \frac{1}{2}\mathbb{Z}_{\geq 0} \\ \hat{h}_{x-1/2} \neq \hat{h}_{x+1/2}}} x.$$

Define the *ground-state path* $\hat{h}^{\text{gs}} \in \mathcal{H}_{\hat{a}, \hat{b}}^p$ to be that path which has minimal weight amongst all the elements of $\mathcal{H}_{\hat{a}, \hat{b}}^p$. It is easily seen that this path has the following shape: an oscillating part having $\hat{h}_x^{\text{gs}} = \hat{b}$ and $\hat{h}_{x+1/2}^{\text{gs}} = \hat{b} - 1/2$ for $x \in \mathbb{Z}_{\geq |\hat{a} - \hat{b}|}$, preceded by an initial straight line having $\hat{h}_x^{\text{gs}} = (\hat{a}, \hat{a} \pm 1/2, \hat{a} \pm 1, \dots, \hat{b} \mp 1/2)$ for $x = (0, 1/2, 1, \dots, |\hat{a} - \hat{b}| - 1/2)$, where the upper signs apply when $\hat{b} \geq \hat{a}$ and the lower signs apply when $\hat{b} < \hat{a}$.

The weight $\widehat{wt}(\hat{h})$ of each $\hat{h} \in \mathcal{H}_{\hat{a}, \hat{b}}^p$ is then defined by

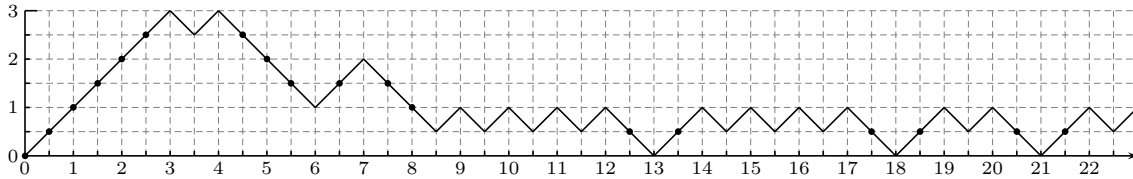
$$(8) \quad \widehat{wt}(\hat{h}) = \hat{w}^\circ(\hat{h}) - \hat{w}^\circ(\hat{h}^{\text{gs}}).$$

For instance, in the path $\hat{h} \in \mathcal{H}_{0,1}^4$ of Fig. 2, we have used dots to indicate the vertices that contribute to (7). The corresponding ground-state path $\hat{h}^{\text{gs}} \in \mathcal{H}_{0,1}^4$ has $\hat{h}_x^{\text{gs}} = 1$ for $x \in \mathbb{Z}_{> 0}$

and $\hat{h}_x^{\text{gs}} = 1/2$ for $x \in \mathbb{Z}_{\geq 0} + 1/2$. Therefore, from (8), we obtain:

$$(9) \quad \widehat{wt}(\hat{h}) = \frac{1}{2} \left(0 + \frac{1}{2} + 1 + \frac{3}{2} + 2 + \frac{5}{2} + \frac{9}{2} + 5 + \frac{11}{2} + \frac{13}{2} + \frac{15}{2} + 8 + \frac{25}{2} + \frac{27}{2} + \frac{35}{2} + \frac{37}{2} + \frac{41}{2} + \frac{43}{2} \right) - \frac{1}{2} \left(0 + \frac{1}{2} \right) = 74.$$

Figure 2: A typical path $\hat{h} \in \mathcal{H}_{0,1}^4$. The black dots indicate the vertices that contribute to the weight, with that at position (x, \hat{h}_x) contributing $x/2$.



In what follows, we make use of the following trick to calculate $\widehat{wt}(\hat{h})$ directly from the path picture of $\hat{h} \in \mathcal{H}_{\hat{a},\hat{b}}^p$. First note that the minimal weight path $\hat{h}^{\text{gs}} \in \mathcal{H}_{\hat{a},\hat{b}}^p$ extends between heights \hat{a} and \hat{b} in its first $2e$ (half-integer) steps, where $e = |\hat{a} - \hat{b}|$. An alternative to (8) for obtaining $\widehat{wt}(\hat{h})$, is to extend \hat{h} to the left by $2e$ steps, in such a way that $\hat{h}_{-e} = \hat{b}$ (overriding the above convention for $\hat{h}_{-1/2}$). The renormalised weight $\widehat{wt}(\hat{h})$ is then obtained by summing the x -coordinates of all the straight vertices of this extended path, beginning with its first vertex at $(-e, \hat{b})$ whose nature is specified by setting $\hat{h}_{-e-1/2} = \hat{b} - 1/2$, and dividing by 2.

Figure 3: A path $\hat{h} \in \mathcal{H}_{3,1}^5$ (solid) and the corresponding ground state \hat{h}^{gs} (dotted).

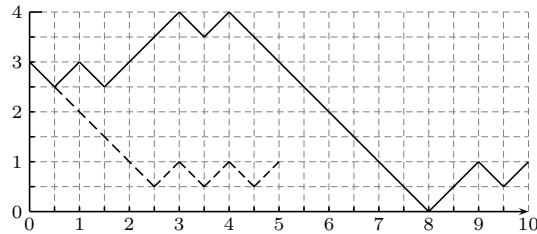
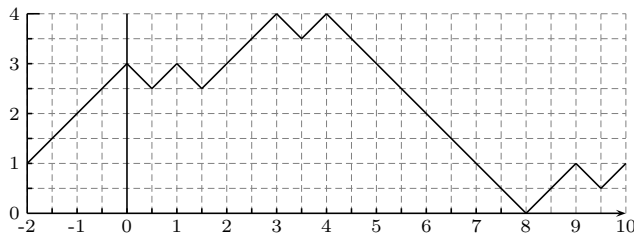


Figure 4: The extension of the path \hat{h} of Fig. 3.



To illustrate this construction, consider the path $\hat{h} \in \mathcal{H}_{3,1}^5$ represented by the solid line in Fig. 3. The minimal weight path $\hat{h}^{\text{gs}} \in \mathcal{H}_{3,1}^5$ is shown dashed. Using (7) and (8), we obtain

$$(10) \quad \begin{aligned} \hat{w}^\circ(\hat{h}) &= \frac{1}{2}(2 + \frac{5}{2} + \frac{9}{2} + 5 + \frac{11}{2} + 6 + \frac{13}{2} + 7 + \frac{15}{2} + \frac{17}{2}) = \frac{55}{2}, \\ \hat{w}^\circ(\hat{h}^{\text{gs}}) &= \frac{1}{2}(\frac{1}{2} + 1 + \frac{3}{2} + 2) = \frac{7}{2} \quad \implies \quad \widehat{wt}(\hat{h}) = \frac{55}{2} - \frac{7}{2} = 24. \end{aligned}$$

Alternatively, we may use the extended path shown in Fig. 4. From this, the renormalised weight $\widehat{wt}(\hat{h})$ is immediately obtained via

$$(11) \quad \widehat{wt}(\hat{h}) = \frac{1}{2}(-2 - \frac{3}{2} - 1 - \frac{1}{2} + 2 + \frac{5}{2} + \frac{9}{2} + 5 + \frac{11}{2} + 6 + \frac{13}{2} + 7 + \frac{15}{2} + \frac{17}{2}) = 24.$$

In [15], the generating function for these paths was conjectured to be a Virasoro character:

$$(12) \quad \sum_{\hat{h} \in \mathcal{H}_{\hat{a}, \hat{b}}^p} q^{\widehat{wt}(\hat{h})} = \chi_{r,s}^{p, 2p+1}(q),$$

where the module labels r, s are given by

$$(13) \quad s = 2\hat{a} + 1 \quad \text{and} \quad r = \hat{b}.$$

2.4. Statement of the results. In the following two sections, we describe a weight-preserving bijection between the sets

$$(14) \quad \mathcal{P}_{a,b}^{p, 2p+1} \leftrightarrow \mathcal{H}_{\frac{1}{2}(a-1), \frac{1}{2}(b-1)}^p,$$

for $p \geq 2$, and a and b odd integers with $1 \leq a < 2p$ and $3 \leq b < 2p$.

In combination with the $p' = 2p + 1$ case of (6), the establishment of this bijection proves (12). Note that for the two sets related by (14), the values of the module labels r and s , obtained for the two cases using (5) and (13) respectively, are in agreement.

At first sight, the restriction on the parity of the values of a and b appears to constrain the applicability of our construction to those modules which are labelled by (r, s) with s odd. However, the equivalence of the modules labelled by (r, s) and $(p - r, p' - s)$ (a consequence of the identity $h_{r,s} = h_{p-r, p'-s}$ for conformal dimensions) implies that, in this $p' = 2p + 1$ case, the construction applies to all inequivalent modules.

In what follows, it is notationally convenient to make the identification

$$(15) \quad \mathcal{P}_{a,b}^p \equiv \mathcal{P}_{a,b}^{p, 2p+1}.$$

3. THE COMBINATORIAL BIJECTION

The description of the bijection given in this section is combinatorial because it is specified in terms of direct manipulations of the paths. This contrasts with the second description, presented in the next section, which is formulated in terms of (non-local) operators. Roughly, in the combinatorial scheme, a path from $\mathcal{P}_{a,b}^p$ is transformed by first stripping off its (charge 1) particles, then reinterpreting the cut path as a $\mathcal{H}_{\hat{a}, \hat{b}}^p$ path through rescaling it by a factor of $1/2$, and finally, reinserting the particles in a precise way.

Throughout this section, we take a and b to be odd integers, with $1 \leq a < 2p$ and $3 \leq b < 2p$, and set

$$(16) \quad \hat{a} = \frac{1}{2}(a - 1) \quad \text{and} \quad \hat{b} = \frac{1}{2}(b - 1).$$

3.1. Specifying the bijection. Let $h \in \mathcal{P}_{a,b}^p$. From h , repeatedly remove adjacent pairs of scoring vertices, in each case adjoining the loose ends (which will be at the same height), until no adjacent pair of scoring vertices remains. Let h^{cut} denote the resulting path. For the path $h \in \mathcal{P}_{1,3}^4$ given in Fig. 1, the resulting $h^{\text{cut}} \in \mathcal{P}_{1,3}^4$ is given in Fig. 5, having removed $n = 4$ pairs of scoring vertices from the former.

To describe the bijection, it is also required that, when carrying out the above removal process, we record the number of non-scoring vertices to the left of each pair of scoring vertices that is removed. This resulting list of n integers then encodes a partition, of at

is determined by setting its parts to be the numberings of the integer valleys amongst all valleys, counted from the left. The parts of μ are necessarily distinct, and thus a genuine partition λ is recovered via (17). That the map $h \rightarrow \hat{h}$ is weight-preserving is demonstrated below.

3.2. Removing basic particles from the RSOS paths⁷. Each pair of adjacent scoring vertices (which are necessarily of different types) in $h \in \mathcal{P}_{a,b}^p$ is identified with a particle:⁸ where there occur $d \geq 2$ consecutive scoring vertices, we identify $\lfloor d/2 \rfloor$ particles (when d is odd, the ambiguity over which pairs are the actual particles is immaterial). The excitation of each of these particles is defined to be the number of non-scoring vertices to its left. Thus, the partition $\lambda(h)$, defined in Section 3.1, lists the excitations of the particles in h .

A path which contains no particles is said to be *particle-deficient*. We construct the particle-deficient path $h^{\text{cut}} \in \mathcal{P}_{a,b}^p$ simply by removing all of the particles from $h \in \mathcal{P}_{a,b}^p$. To determine the weight of h^{cut} , first consider the removal of one such particle from h . Let λ_i be the number of non-scoring vertices to its left, and let k be the total number of scoring vertices in h ($k = 13$ for the path of Fig. 1). The band structure for the $p' = 2p + 1$ cases ensures that the first of the two scoring vertices that comprise the particle is necessarily a peak or valley. Let it be at position (x, h_x) . If it is a peak, then the following vertex is at $(x + 1, h_x - 1)$, and together they contribute

$$(18) \quad u_x + v_{x+1} = \frac{1}{2}(x - h_x + a + x + 1 + h_x - 1 - a) = x$$

to the weight. If it is a valley, then the following vertex is at $(x + 1, h_x + 1)$, and together they contribute

$$(19) \quad v_x + u_{x+1} = \frac{1}{2}(x + h_x - a + x + 1 - h_x - 1 + a) = x$$

to the weight. There are $x - 1 - \lambda_i$ scoring vertices to the left of the particle, and thus $\lambda_i + k - x - 1$ to its right. On removing the particle, the contribution of each of the latter to the weight decreases by one. Thus the total weight reduction on removing the particle is $\lambda_i + k - 1$.

Then, if h contains n particles, on removing all of them, noting that k decreases by two at each step, we obtain

$$(20) \quad \begin{aligned} wt(h^{\text{cut}}) &= wt(h) - \sum_{i=1}^n \lambda_i - (k - 1) - (k - 3) - (k - 5) - \dots - (k - 2n - 1) \\ &= wt(h) - \sum_{i=1}^n \lambda_i - n(k - n). \end{aligned}$$

3.3. Mapping from RSOS paths to half-lattice paths. Given a particle-deficient path $h^{\text{cut}} \in \mathcal{P}_{a,b}^p$, define a half-lattice path \hat{h}^{cut} by shrinking h^{cut} by a factor of 2, and decreasing all heights by 1/2. Note that \hat{h}^{cut} is a element of $\mathcal{H}_{a,b}^p$, whose valleys are at non-integer heights. In this section, we show that $\widehat{wt}(\hat{h}^{\text{cut}}) = wt(h^{\text{cut}})$.

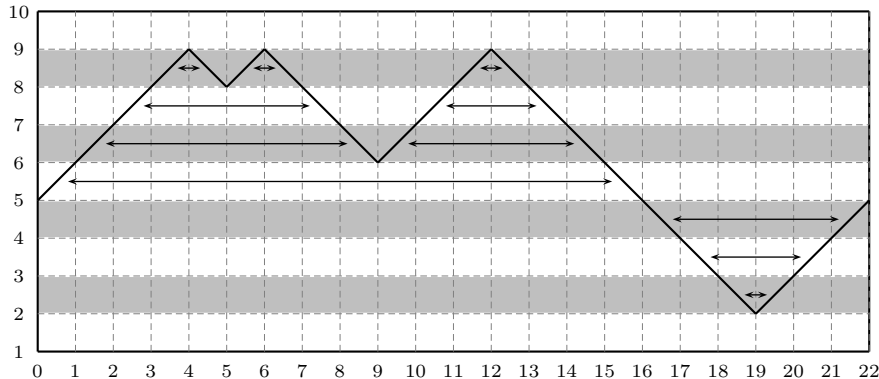
First consider the case where $a = b$. (The path h^{cut} then starts and ends at the same height — if truncated beyond the start of the final oscillation). In such a case, we may match (pair) each path segment with another at the same height, one NE and one SE (the order is immaterial). This matching process is illustrated in Fig. 7.

Since h^{cut} has no peak at an even height and no valley at an odd height, the scoring vertices of h^{cut} occur at the right ends of all the segments in the light bands. Consider a specific matched pair of segments in a light band, with the left ends of the NE and

⁷ The process presented in this section is described, using similar terminology, in [22, Section 5] (cf. eqn. (15) therein), and previously in [7, Section 2] using the notions of \mathcal{B}_2 and \mathcal{B}_3 transforms (therein, $h^{(0)}$ is used to denote h^{cut}).

⁸These are the particles of charge 1 in the terminology of [16].

Figure 7: Example of segment matching for a path h .



SE segments at positions (x, y) and $(x', y + 1)$ respectively. The two scoring vertices at $(x + 1, y + 1)$ and $(x' + 1, y)$ together contribute

$$(21) \quad u_{x+1} + v_{x'+1} = \frac{1}{2}(x + 1 - (y + 1) + a + x' + 1 + y - a) = \frac{1}{2}(x + x' + 1)$$

to $wt(h^{\text{cut}})$.

For the corresponding half-lattice path \hat{h}^{cut} , the weight may be obtained by considering the four straight vertices at each end of each of the segments of the matched pair (the vertex at $(0, \hat{a})$ will be required here if it's straight). These four vertices contribute

$$(22) \quad \frac{1}{2} \left[\frac{1}{2}x + \frac{1}{2}(x + 1) + \frac{1}{2}x' + \frac{1}{2}(x' + 1) \right] = \frac{1}{2}(x + x' + 1)$$

to $\hat{w}^\circ(\hat{h}^{\text{cut}})$. Since this agrees with the contribution of the corresponding two scoring vertices of h^{cut} to the weight $wt(h^{\text{cut}})$, we conclude that $\hat{w}^\circ(\hat{h}^{\text{cut}}) = wt(h^{\text{cut}})$. But, for $a = b$, $\widehat{wt}(\hat{h}^{\text{cut}}) = \hat{w}^\circ(\hat{h}^{\text{cut}})$, thereby proving that $\widehat{wt}(\hat{h}^{\text{cut}}) = wt(h^{\text{cut}})$ in this $a = b$ case.

In the case that $a \neq b$, we make use of the trick described in Section 2.3 to obtain $\widehat{wt}(\hat{h}^{\text{cut}})$ by extending the path \hat{h}^{cut} to the left. On the other hand, extending the path h^{cut} to the left by $2e = |a - b|$ steps with $h_{-2e}^{\text{cut}} = b$, creates a path of unchanged weight $wt(h^{\text{cut}})$ because, via (1), the additional scoring vertices each contribute 0 to the weight. Then, upon applying the argument used above in the $a = b$ case to these extended paths, we obtain $\widehat{wt}(\hat{h}^{\text{cut}}) = wt(h^{\text{cut}})$ for $a \neq b$ also.

3.4. Deepening valleys. Consider a half-lattice path $\hat{h}^{(0)} \in \mathcal{H}_{\hat{a}, \hat{b}}^p$, having m straight vertices. This count includes consideration of the vertex at $(0, \hat{a})$, which, through the convention stated in Section 2.3, is deemed straight if and only if the first segment of $\hat{h}^{(0)}$ is in the NE direction. The vertices of $\hat{h}^{(0)}$ that do not contribute to its weight are the peaks and valleys. We now determine the change in weight on deepening one of the valleys. Let the valley being deepened be the j th, counting from the left, and let it be situated at $(x, \hat{h}_x^{(0)})$. There are necessarily j peaks to the left of this valley (perhaps including one at $(0, \hat{a})$), and therefore $2x + 1 - 2j$ straight vertices. After this position, there are thus $m - 2x + 2j - 1$ straight vertices. The deepening moves each of these to the right by two (half-integer) positions. It also introduces two straight vertices, at positions $(x, \hat{h}_x^{(0)})$ and $(x + 1, \hat{h}_x^{(0)})$. Thus, if this

resulting path is denoted $\hat{h}^{(1)}$,

$$\begin{aligned} \widehat{wt}(\hat{h}^{(1)}) &= \widehat{wt}(\hat{h}^{(0)}) + \frac{1}{2}(x + (x + 1)) + \frac{1}{2}(m - 2x + 2j - 1) \\ (23) \qquad \qquad &= \widehat{wt}(\hat{h}^{(0)}) + \frac{1}{2}m + j. \end{aligned}$$

Note that the deepening increases the value of m by 2. So if we obtain the path \hat{h} by performing a succession of deepening to a path \hat{h}^{cut} at valleys numbered $\mu_1, \mu_2, \dots, \mu_n$, we have

$$\begin{aligned} \widehat{wt}(\hat{h}) &= \widehat{wt}(\hat{h}^{\text{cut}}) + \frac{1}{2}(m + (m + 2) + \dots + (m + 2n - 2)) + \sum_{i=1}^n \mu_i \\ (24) \qquad \qquad &= \widehat{wt}(\hat{h}^{\text{cut}}) + \frac{n}{2}(m + n - 1) + \sum_{i=1}^n \mu_i. \end{aligned}$$

3.5. Altogether now. Consider the combined map $h \rightarrow (h^{\text{cut}}, n, \lambda) \rightarrow (\hat{h}^{\text{cut}}, n, \mu) \rightarrow \hat{h}$ defined in Section 3.1 above. Let k and k' be the number of scoring vertices in h and h^{cut} respectively, and let m be the number of straight vertices (including consideration of the vertex at $(0, \hat{a})$ in \hat{h}^{cut}). The pair removal process in Section 3.2 shows that $k' = k - 2n$. The matching of edges described in Section 3.3 shows that $m = 2k'$ and thus $m = 2k - 4n$. Then, using eqns. (20) and (24), and the fact that $\widehat{wt}(\hat{h}^{\text{cut}}) = wt(h^{\text{cut}})$, we obtain

$$\begin{aligned} \widehat{wt}(\hat{h}) - wt(h) &= \sum_{i=1}^n \mu_i - \sum_{i=1}^n \lambda_i + \frac{n}{2}(m + n - 1) - n(k - n) \\ (25) \qquad \qquad &= \sum_{i=1}^n \mu_i - \sum_{i=1}^n \lambda_i - \frac{n}{2}(n + 1) \\ &= 0, \end{aligned}$$

where the final equality follows because, using (17),

$$(26) \qquad \sum_{i=1}^n \mu_i - \sum_{i=1}^n \lambda_i = \sum_{i=1}^n i = \frac{n}{2}(n + 1).$$

Thus the weight-preserving nature of the bijection has been proved.

4. THE PATH-OPERATOR BIJECTION

In this section, we introduce natural descriptions of each of the two types of paths in terms of sequences of (local and non-local) operators. In the case of the RSOS paths $\mathcal{P}_{a,b}^p$, these sequences are encodings of the vertex words introduced in [22]. For the $\mathcal{H}_{\hat{a},\hat{b}}^p$ paths, the sequences are simplified versions of a modification of those already presented in [14]. The bijection between $\mathcal{P}_{a,b}^p$ and $\mathcal{H}_{\hat{a},\hat{b}}^p$, described in the previous section, is then formulated as a rule for transforming between such sequences.

4.1. \mathcal{P}^p paths as sequences of operators. For each path $h \in \mathcal{P}_{a,b}^{p,p'}$, the vertex word $w(h)$ is defined to be the sequence of letters S and N which indicate the sequence of vertices, scoring or non-scoring, of h , read from the left [22, §5]. For example, for the path h given in Fig. 1,

$$(27) \qquad w(h) = SNSSSNNSNNSSNSNNSNSSSNNNNNNNNNNNN \dots$$

Each vertex word $w(h)$ is of infinite length and, because the tail of h lies in a dark band, $w(h)$ contains only a finite number of letters S . As indicated in [22], every infinite length word w in S and N having only finite number of entries S , is the vertex word $w = w(h)$ of at most one path h .

In the cases where $p' = 2p + 1$, and a and b are odd integers with $1 \leq a < 2p$ and $3 \leq b < 2p$, we encode $w(h)$ as follows. After indexing the letters of the vertex word of $w(h)$ by the x -coordinates of the corresponding vertices, drop all letters N . Then, reading from the left, replace each consecutive pair $S_{x+1}S_{x+2}$ by d_x . Then replace each remaining S_{y+1} by c_y or c_y^* depending on whether y is even or odd. This yields a finite sequence of *symbols* d_x , c_y and c_z^* which uniquely represents the original path h . We denote it $\pi(h)$ and refer to it as the *operator word* of h . In the case of the path h of Fig. 1, from (27), we obtain

$$(28) \quad \pi(h) = c_0 d_2 c_4 c_6 d_{10} c_{13}^* d_{16} d_{19} c_{21}^*.$$

Each symbol d_x , c_y or c_z^* may be viewed as an operator which changes the nature of three or two vertices of an oscillating portion of a path near position x , y or z respectively. These actions are illustrated in Fig. 8. The path h then results from the action of the operator word $\pi(h)$ on the purely oscillating *vacuum path* $h^{\text{vac}(b)} \in \mathcal{P}_{b,b}^p$, defined by $h_x^{\text{vac}(b)} = b$ for x even and $h_x^{\text{vac}(b)} = b - 1$ for x odd.

Note that the operator d_x acts locally to generate either a peak or a valley in a light band, changing neither the path's startpoint nor tail. In contrast, the actions of the operators c_x and c_x^* are non-local in the sense that they change the portion of the path lying between 0 and $x + 1$. In particular, they change the startpoint of the path, decreasing and increasing it by 2 respectively.⁹

Therefore, because the operator word $\pi(h)$ maps between elements of $\mathcal{P}_{b,b}^p$ and $\mathcal{P}_{a,b}^p$, it follows that the difference between the number of operators c_y and c_z^* in the operator word $\pi(h)$ is $(b - a)/2$.

Obtained as described above, the subscripts of neighbouring pairs of operators in $\pi(h)$ naturally satisfy certain constraints. They are:

$$(29) \quad \begin{aligned} d_x c_{x'}^{(*)}, c_x^{(*)} d_{x'}, d_x d_{x'}, c_x c_{x'}, c_x^* c_{x'}^* &\implies x' \geq x + 2, \\ c_x c_{x'}^*, c_x^* c_{x'} &\implies x' \geq x + 3, \end{aligned}$$

where $c^{(*)}$ denotes either c or c^* . A word π in the symbols d_x , c_y , c_z^* is called *standard* if every neighbouring pair in π respects the constraints (29).

In the operator word $\pi(h)$, the particles described in Section 3.2 correspond to the symbols d_x . The excitation of each such particle is given by the number of non-scoring vertices in h to its left. Therefore, for the i th operator d_x in $\pi(h)$, counted from the right, this excitation is given by

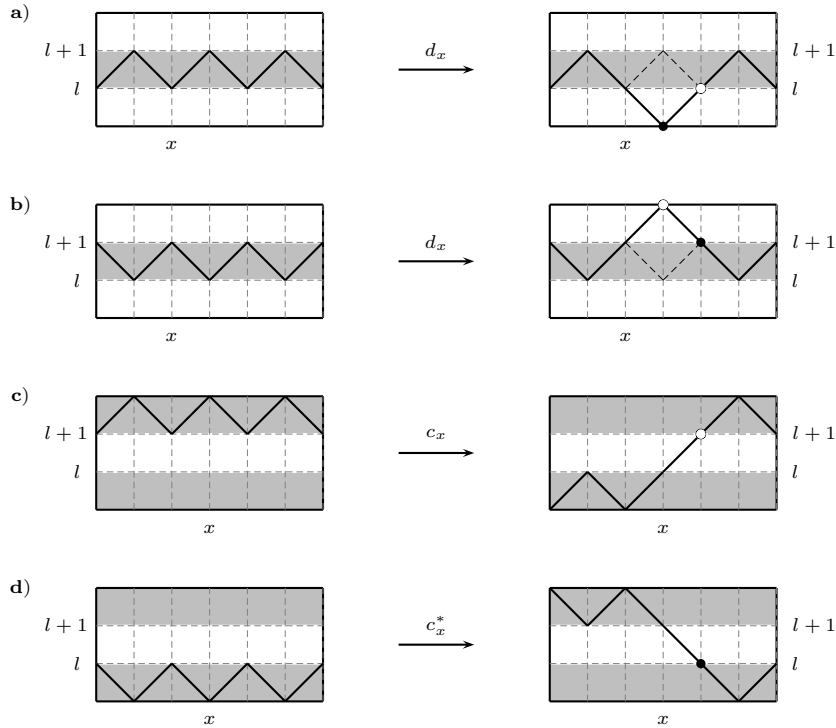
$$(30) \quad \lambda_i = x - 2\#\{d \cdots d_x\} - \#\{c^{(*)} \cdots d_x\},$$

where $\#\{A \cdots B\}$ denotes the number of pairs A and B of operators in $\pi(h)$ with A to the left of B . For instance, consider the excitation λ_1 of the particle corresponding to d_{19} in the word (28): there are three pairs of the first type: (d_2, d_{19}) , (d_{10}, d_{19}) , and (d_{16}, d_{19}) , and four pairs of the second type: (c_0, d_{19}) , (c_4, d_{19}) , (c_6, d_{19}) , and (c_{13}^*, d_{19}) . Thus, in this case, the excitation is $\lambda_1 = 19 - 6 - 4 = 9$.

For an arbitrary word π in the symbols d_x , c_y , c_z^* , we use (30) to define λ_i for the i th operator d_x , counted from the right. Then define the vector $\lambda(\pi) = (\lambda_1, \lambda_2, \dots, \lambda_n)$, where n is the number of operators d_x in π . If $\lambda_1 \geq \lambda_2 \geq \dots \geq \lambda_n \geq 0$ (so that $\lambda(\pi)$ is a partition), then we say that π is *physical*. Otherwise, we say that π is *unphysical*. The constraints (29) guarantee that every standard word $\pi(h)$ is physical.

⁹ The operators c_x and c_x^* map between paths which label states of different modules. Their actions could be defined either to maintain the tail and change the initial point ($\mathcal{P}_{a,b}^p \rightarrow \mathcal{P}_{a \mp 2, b}^p$), as described in the main text, or, alternatively, to change the tail and maintain the initial point ($\mathcal{P}_{a,b}^p \rightarrow \mathcal{P}_{a, b \pm 2}^p$), as in [14] for unitary RSOS paths. Under the action of $c_x^{(*)}$, the paths are then modified either in the interval $[0, x + 1]$, as in the main text, or, alternatively, in the interval $[x, \infty]$. Either choice corresponds to a genuine non-local action. However, the first one is somewhat more localized. This is one motivation for the choice made here. But the ultimate reason lies in the expected greater simplicity of this choice in the treatment of other (than the $p' = 2p + 1$) classes of models.

Figure 8: The action of the operators d_x , c_x and c_x^* on a portion of a path that oscillates in a dark band. Note that d_x either creates a valley (cf. (a)) or a peak (cf. (b)) in a light band according to the odd/even parity of x .



We now consider the effect on $\pi(h)$ of changing the excitations of the particles in h . First consider incrementing or decrementing the excitation of the particle corresponding to an operator d_x . This is possible if and only if we obtain a physical word π' on replacing the operator d_x in $\pi(h)$ by d_{x+1} or d_{x-1} respectively (otherwise, the particle is ‘blocked’: two particles cannot occupy the same position). Even if physical, the word π' might not be standard. However, if standard, the resulting path is readily obtained from π' via the actions given in Fig. 8. If it is not standard, then necessarily we would have made one of the local changes:

$$(31a) \quad d_x c_{x+2}^{(*)} \rightarrow d_{x+1} c_{x+2}^{(*)},$$

$$(31b) \quad c_{x-2}^{(*)} d_x \rightarrow c_{x-2}^{(*)} d_{x-1},$$

depending on whether we incremented or decremented the excitation. These violations of (29) may be seen to arise because, within an odd length sequence of scoring vertices, there is ambiguity over which pairs correspond to the particles. For example, the sequence $NSSSN$ might be interpreted with the first two S s being the particle, thereby yielding the operators $d_1 c_3$, or the latter two S s being the particle, thereby yielding the operators $c_1 d_2$. Thus, we should impose the equivalence

$$(32) \quad d_x c_{x+2}^{(*)} \equiv c_x^{(*)} d_{x+1}.$$

In the case of the moves (31), this equivalence should be applied before increasing the excitation in the case (31a), and after decreasing the excitation in the case (31b).

To excite the particle corresponding to a particular d_x by more than 1, we can proceed as above, one step at a time. However, we easily see that the process can be streamlined by

first adding the required excitement to the subscript of d_x (this excitation being possible if and only if the resulting word is physical), and then for each pair $d_y c_{y'}^{(*)}$ with $y' < y + 2$, imposing the equivalence

$$(33) \quad d_y c_{y'}^{(*)} \equiv c_{y'-2}^{(*)} d_{y+1}.$$

For example, consider the operator word

$$(34) \quad d_0 d_2 d_4 d_6 c_8 c_{10} c_{12} c_{17}^* c_{21}^*.$$

Exciting the rightmost particle (represented by d_6) by 9 yields first

$$(35) \quad d_0 d_2 d_4 d_{15} c_8 c_{10} c_{12} c_{17}^* c_{21}^*.$$

Repeatedly applying (33) yields the following sequence of words:

$$(36) \quad \begin{aligned} d_0 d_2 d_4 (d_{15} c_8) c_{10} c_{12} c_{17}^* c_{21}^* &\rightarrow d_0 d_2 d_4 c_6 (d_{16} c_{10}) c_{12} c_{17}^* c_{21}^* \\ &\rightarrow d_0 d_2 d_4 c_6 c_8 (d_{17} c_{12}) c_{17}^* c_{21}^* \\ &\rightarrow d_0 d_2 d_4 c_6 c_8 c_{10} (d_{18} c_{17}^*) c_{21}^* \\ &\rightarrow d_0 d_2 d_4 c_6 c_8 c_{10} c_{15}^* d_{19} c_{21}^*, \end{aligned}$$

where, in each line, we have used parentheses to indicate the pair of operators affected. Conversely, we can reduce the excitation of a d_x by decreasing its subscript by the required amount (again, this is possible if and only if the resulting word is physical), and then repeatedly using (33) in the cases $y' \geq y + 2$ to reexpress the right side as the left side. In either case, once the standard operator word has been obtained, the corresponding RSOS path can be readily constructed using Fig. 8.

The construction may be applied to excite a number of particles simultaneously. For example, applying the excitations 1, 5, 8 and 9 to the particles of the operator word (34) yields the non-standard word

$$(37) \quad d_1 d_7 d_{12} d_{15} c_8 c_{10} c_{12} c_{17}^* c_{21}^*.$$

It may be checked that repeated use of (33) then yields the standard word given in (28), which corresponds to the path of Fig. 1.¹⁰

Finally, for this section, we note that the excitation of a particle corresponding to an operator d_x in an operator word π is given by (30), even when the word is non-standard. This is so because the value of the expression (30) is unchanged for operator words obtained from one another through the equivalence (33).

4.2. \mathcal{H}^p paths as sequences of operators. Here, we provide an encoding of the half-lattice paths of $\mathcal{H}_{\hat{a}, \hat{b}}^p$ that is analogous to that of the previous section.

For $\hat{a}, \hat{b} \in \mathbb{Z}$, let $\hat{h} \in \mathcal{H}_{\hat{a}, \hat{b}}^p$. Because \hat{h} has no peak at a non-integer height, it follows that if there is a straight-up vertex at position $x \in \mathbb{Z}$, there must also be one at position $x + 1/2$, and if there is a straight-down vertex at position $x \in \mathbb{Z} + \frac{1}{2}$, there must either be a straight-down vertex at position $x + 1/2$ or a straight-up vertex at position $x + 1$. Similarly, if there is a straight-down vertex at position $x \in \mathbb{Z}$, there must also be one at position $x - 1/2$, and if there is a straight-up vertex at position $x \in \mathbb{Z} + \frac{1}{2}$, there must either be a straight-up vertex at position $x - 1/2$ or a straight-down vertex at position $x - 1$. Consequently, working from the left of \hat{h} , we may consecutively pair the straight vertices such that each pair occurs at neighbouring positions x and $x + 1/2$, or next neighbouring positions x and $x + 1$ (through the convention stated in Section 2.3, the vertex at $(0, \hat{a})$ is deemed straight if and only if the first segment of \hat{h} is in the NE direction). We encode each of those pairs that occur at positions x and $x + 1/2$ using \hat{c}_x or \hat{c}_x^* depending on whether x is integer or non-integer

¹⁰Operator words of the form (34) which begin with the n operators $d_0 d_2 d_4 \cdots d_{2n-2}$ are, in the language of [7], the result of a $\mathcal{B}_2(n)$ -transform on a particle-deficient path. The process of exciting these particles corresponds to the $\mathcal{B}_3(\lambda)$ -transform, with the excitation of the i th particle, counted from the right, specified by the part λ_i of the partition λ .

respectively. In the other case, where the pair occurs at positions x and $x + 1$, we encode the pair using \hat{d}_x . In this latter case, note that $x \in \mathbb{Z} + \frac{1}{2}$ and that there is a valley at the intermediate position $x + 1/2$. Let $\hat{\pi}(\hat{h})$ denote the word in the symbols $\hat{d}_x, \hat{c}_y, \hat{c}_z^*$ obtained in this way, ordered with increasing subscripts. We refer to it as the *operator word* of \hat{h} . Of course, the half-lattice path \hat{h} can be immediately recovered from $\hat{\pi}(\hat{h})$.¹¹

To illustrate this construction, consider the path \hat{h} of Fig. 2. Here, the operator word $\hat{\pi}(\hat{h})$ is found to be

$$(38) \quad \hat{\pi}(h) = \hat{c}_0 \hat{c}_1 \hat{c}_2 \hat{c}_9^* \hat{d}_{\frac{11}{2}} \hat{c}_{\frac{15}{2}}^* \hat{d}_{\frac{25}{2}} \hat{d}_{\frac{35}{2}} \hat{d}_{\frac{41}{2}}.$$

Each symbol \hat{d}_x, \hat{c}_y or \hat{c}_z^* may be viewed as an operator which changes the nature of two vertices of an oscillating portion of a path near position x, y or z respectively. These actions are illustrated in Fig. 9. The path \hat{h} then results from the action of the operator word $\hat{\pi}(\hat{h})$ on the purely oscillating *vacuum path* $\hat{h}^{\text{vac}(\hat{b})} \in \mathcal{H}_{\hat{b}, \hat{b}}^p$, defined by $\hat{h}_x^{\text{vac}(\hat{b})} = \hat{b}$ and $\hat{h}_{x+1/2}^{\text{vac}(\hat{b})} = \hat{b} - 1/2$ for $x \in \mathbb{Z}_{\geq 0}$.

Note that the actions of the operators \hat{c}_y and \hat{c}_z^* are non-local in the sense that they change the starting height of the path, decreasing and increasing it by 1 respectively. In contrast, \hat{d}_x does not affect the path's starting point, acting locally to change an integer peak into an integer valley.

The subscripts of the symbols in the word $\hat{\pi}(\hat{h})$ naturally satisfy certain constraints. They are:

$$(39) \quad \begin{aligned} \hat{c}_x \hat{c}_{x'}, \hat{c}_x^* \hat{c}_{x'}, \hat{c}_x^* \hat{d}_{x'} &\implies x' \geq x + 1, \\ \hat{c}_x^* \hat{c}_{x'}, \hat{c}_x \hat{c}_{x'}, \hat{d}_x \hat{c}_{x'}, \hat{c}_x \hat{d}_{x'} &\implies x' \geq x + \frac{3}{2}, \\ \hat{d}_x \hat{d}_{x'}, \hat{d}_x \hat{c}_{x'} &\implies x' \geq x + 2. \end{aligned}$$

¹¹ As mentioned in the introduction of the section, this operator construction of the \mathcal{H}^p paths is a modified version of the one already presented in [14]. To substantiate this statement, let us recall briefly the operator construction of \mathcal{H}^p paths in [14]. The paths are constructed from the appropriate ground state by the action of a sequence of non-local operators b_x, b_x^* : b_x transforms a peak at x into a straight-up segment and b_x^* transforms a valley at x into a straight-down segment (both segments linking the points x and $x + 1/2$). These actions modify the path for all $x' \geq x + 1/2$ (in contradistinction with the actions of the operators defined in the main text, which are limited to the initial portion of the path, namely $x' \leq x$). The constraint on the integrality of the peak positions shows that the operators b and b^* always occur in successive pairs that are either of the types (bb) , (b^*b^*) or (b^*b) , with subindices differing by a half-integer in the first two cases and by an integer in the third one. In terms of these operators, the operators \tilde{c}, \tilde{c}^* and \hat{d} are expressed

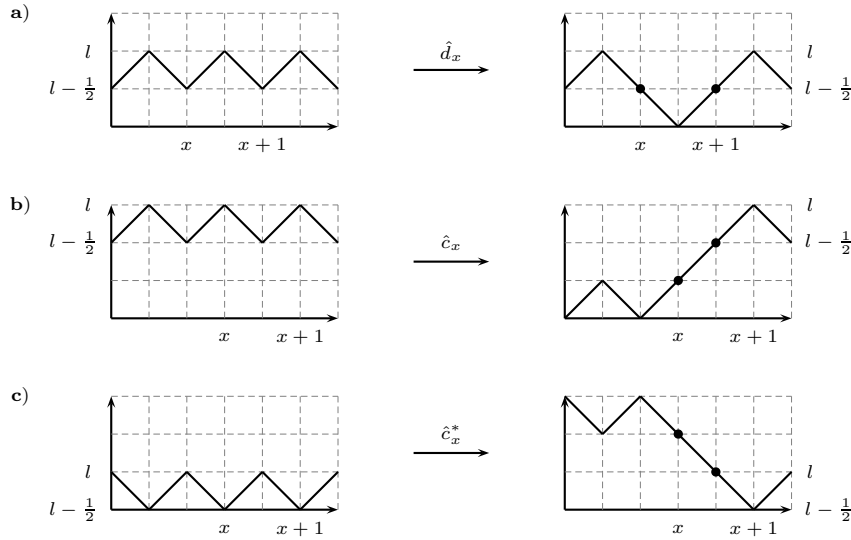
$$\tilde{c}_x = b_x b_{x+1/2}, \quad \tilde{c}_{x'}^* = b_{x'}^* b_{x'+1/2}^*, \quad \hat{d}_{x'} = b_{x'}^* b_{x'+1}.$$

\hat{d} is the same as the operator defined in the main text, while \tilde{c} and \tilde{c}^* are roughly the operators \hat{c} and \hat{c}^* but acting instead to maintain the path's initial portion, while changing its tail. Summing up, our present operator construction is different from that introduced in [14] in two ways: it uses a reduced number of operators and the operator action modifies the initial rather than the final portion of the path. Let us now turn to the interpretation where particles are viewed as the path's basic constituents [21, 14, 16]. Given that every path is described by a sequence composed of an equal number of operators b and b^* , it can be seen, from the decomposition of a path into charged peaks [15], that there are actually $2p - 3$ combinations of the b and b^* that are allowed. These are the l -blocks — the particles whose numbers are the summation variables in the fermionic character — defined by [14]:

$$b^{l-1} b^* l b \text{ for } l \text{ odd and } b^l b^* l \text{ for } l \text{ even, where } 1 \leq l \leq 2p - 3.$$

In terms of the new operators, the path building blocks are seen to be simply the $p - 1$ combinations: \hat{d} and $\tilde{c}^\ell \tilde{c}^{*\ell}$, or equivalently $\hat{c}^\ell \hat{c}^{*\ell}$, for $1 \leq \ell \leq p - 2$. (In the terminology of [16], these particles are interpreted as a breather and pairs of kinks-antikinks of topological charge ℓ respectively.) This particle interpretation is the starting point for a direct derivation of the characters (in the line of [21]) that matches the usual expressions given in [17, 3, 8, 7, 23, 16].

Figure 9: The action of the operators \hat{d}_x , \hat{c}_x and \hat{c}_x^* on a portion of a path that oscillates between heights l and $l - 1/2$, where $l \in \mathbb{Z}$. The black dots are the vertices that contribute to the weight.



Later, we consider arbitrary words in the operators \hat{d}_x , \hat{c}_y and \hat{c}_z^* , with each $y \in \mathbb{Z}$ and each $x, z \in \mathbb{Z} + \frac{1}{2}$. Such a word $\hat{\pi}$ is called *standard* if every neighbouring pair in $\hat{\pi}$ respects the constraints (39).

Each operator \hat{d}_x in $\hat{\pi}(\hat{h})$ corresponds to an integer valley of \hat{h} at position $x + 1/2 \in \mathbb{Z}$. We define the excitation of this integer valley to be the number of non-integer valleys to its left. To express this excitation in terms of the operator word $\hat{\pi}(\hat{h})$, let $\#\{A \cdots B\}$ denote the number of pairs A and B of operators in $\hat{\pi}(\hat{h})$ with A to the left of B . The number of straight vertices strictly to the left of position $x + 1$ is then $2\#\{\hat{d} \cdots \hat{d}_x\} + 2\#\{\hat{c}^{(*)} \cdots \hat{d}_x\} + 1$, where $\hat{c}^{(*)}$ denotes either \hat{c} or \hat{c}^* (the $+1$ accounting for the straight-down vertex of \hat{d}_x at x). Thus, the number of valleys and peaks strictly to the left of $x + 1$ is $2x + 1 - 2\#\{\hat{d} \cdots \hat{d}_x\} - 2\#\{\hat{c}^{(*)} \cdots \hat{d}_x\}$. Exactly half of these are valleys. Of those, $\#\{\hat{d} \cdots \hat{d}_x\} + 1$ are integer valleys. Therefore, the excitation of the integer valley corresponding to the i th operator \hat{d}_x in $\hat{\pi}(\hat{h})$, counted from the right, is given by

$$(40) \quad \hat{\lambda}_i = x - \frac{1}{2} - 2\#\{\hat{d} \cdots \hat{d}_x\} - \#\{\hat{c}^{(*)} \cdots \hat{d}_x\}.$$

Proceeding as in Section 4.1, for an arbitrary word $\hat{\pi}$ in the symbols \hat{d}_x , \hat{c}_y , \hat{c}_z^* , we use (40) to define $\hat{\lambda}_i$ for the i th operator \hat{d}_x , counted from the right. Then define the vector $\hat{\lambda}(\hat{\pi}) = (\hat{\lambda}_1, \hat{\lambda}_2, \dots, \hat{\lambda}_n)$, where n is the number of operators \hat{d}_x in $\hat{\pi}$. If $\hat{\lambda}_1 \geq \hat{\lambda}_2 \geq \dots \geq \hat{\lambda}_n \geq 0$ then we say that $\hat{\pi}$ is *physical*, and *unphysical* otherwise. Again, the constraints (39) ensure that every standard word $\hat{\pi}(\hat{h})$ is physical.

We now consider the effect on $\hat{\pi}(\hat{h})$ of changing the excitations of the particles in \hat{h} , mirroring the analysis of the previous section with some adjustments. First consider incrementing the excitation of the integer valley corresponding to an operator \hat{d}_x . This is possible if and only if we obtain a physical word $\hat{\pi}'$ on replacing the operator \hat{d}_x in $\hat{\pi}(\hat{h})$ by \hat{d}_{x+1} (otherwise, the integer valley is ‘blocked’). Here again, even if physical, the word $\hat{\pi}'$ might not be standard.

The effect on \hat{h} of incrementing the excitation is to make shallower the valley of \hat{h} at position $x + 1/2$, and to deepen the subsequent valley. Let \hat{h}' be the resulting path. We

claim that if $\hat{\pi}'$ is standard then $\hat{\pi}(\hat{h}') = \hat{\pi}'$. This is so because, if $\hat{\pi}'$ is standard then, in $\hat{\pi}(\hat{h})$, the operator \hat{d}_x is immediately followed by either an operator $\hat{c}_{x'}^{(*)}$ or an operator $\hat{d}_{x'}$ (or nothing) with $x' > x + 2$. Thus, the subsequent valley to be deepened is at position $x + 2$. We then see that $\hat{\pi}(\hat{h}') = \hat{\pi}'$, as claimed.

On the other hand, if $x' \leq x + 2$, the word $\hat{\pi}'$ is non-standard. In this case, we ascertain the position of the subsequent valley in \hat{h} from the sequence of operators that follow \hat{d}_x in $\hat{\pi}(\hat{h})$. In this word, \hat{d}_x and subsequent operators necessarily form the standard subword

$$(41) \quad \hat{d}_x \hat{c}_{x+3/2} \hat{c}_{x+5/2} \cdots \hat{c}_{x+t+1/2} \hat{c}_{x+t+2}^* \hat{c}_{x+t+3}^* \cdots \hat{c}_{x+t+t^*+1}^*,$$

where $t \geq 0$, $t^* \geq 0$, with at least one of these non-zero, and any subsequent operators have subscripts at least $x + t + t^* + 5/2$ (there cannot be a subsequent operator \hat{d}_{x+t+t^*+2} because, as is readily checked using (40), with such an operator, the word $\hat{\pi}'$ would be unphysical). The subsequent valley is then at position $x + t + t^* + 2$. Therefore, the word $\hat{\pi}(\hat{h}')$ is obtained from $\hat{\pi}(\hat{h})$ by replacing the subword (41) by

$$(42) \quad \hat{c}_{x+1/2} \hat{c}_{x+3/2} \cdots \hat{c}_{x+t-1/2} \hat{c}_{x+t+1}^* \hat{c}_{x+t+2}^* \cdots \hat{c}_{x+t+t^*}^* \hat{d}_{x+t+t^*+1}.$$

Alternatively, we may proceed in a similar way to that in Section 4.1, using non-standard words. Then, to effect the excitement, first increment the subscript of \hat{d}_x in $\hat{\pi}(\hat{h})$, regardless of subsequent operators. The excitement is possible if the resulting word $\hat{\pi}'$ is physical. Then, if the word is standard, it is $\hat{\pi}(\hat{h}')$. Otherwise, a subword of the form (41) must have been present in $\hat{\pi}(\hat{h})$. We then proceed by imposing the equalities

$$(43a) \quad \hat{d}_y \hat{c}_{y+1/2} \equiv \hat{c}_{y-1/2} \hat{d}_{y+1},$$

$$(43b) \quad \hat{d}_y \hat{c}_{y+1}^* \equiv \hat{c}_y^* \hat{d}_{y+1},$$

until a standard word results. This standard word is $\hat{\pi}(\hat{h}')$ because, after replacing \hat{d}_x by \hat{d}_{x+1} in (41), this procedure produces (42).

As in Section 4.1, we can streamline the process of exciting a particular \hat{d}_x , by adding the required excitation to the subscript (this excitation being possible if and only if the resulting word is physical) and then repeatedly imposing

$$(44) \quad \hat{d}_y \hat{c}_{y'}^{(*)} \equiv \hat{c}_{y'-1}^{(*)} \hat{d}_{y+1},$$

until the word is standard.

For example, consider the standard word

$$(45) \quad \hat{c}_1 \hat{c}_2 \hat{d}_{\frac{7}{2}} \hat{c}_{\frac{11}{2}}^* \hat{c}_8 \hat{c}_{\frac{19}{2}}^* \hat{c}_{\frac{21}{2}}^* \hat{c}_{14}.$$

Increasing the excitation of the $\hat{d}_{\frac{7}{2}}$ by 5, and standardising the resulting non-standard word using (44), results in the sequence:

$$(46) \quad \begin{aligned} \hat{c}_1 \hat{c}_2 (\hat{d}_{\frac{17}{2}} \hat{c}_{\frac{11}{2}}^*) \hat{c}_8 \hat{c}_{\frac{19}{2}}^* \hat{c}_{\frac{21}{2}}^* \hat{c}_{14} &\rightarrow \hat{c}_1 \hat{c}_2 \hat{c}_{\frac{9}{2}}^* (\hat{d}_{\frac{19}{2}} \hat{c}_8) \hat{c}_{\frac{19}{2}}^* \hat{c}_{\frac{21}{2}}^* \hat{c}_{14} \\ &\rightarrow \hat{c}_1 \hat{c}_2 \hat{c}_{\frac{9}{2}}^* \hat{c}_7 (\hat{d}_{\frac{21}{2}} \hat{c}_{\frac{19}{2}}^*) \hat{c}_{\frac{21}{2}}^* \hat{c}_{14} \\ &\rightarrow \hat{c}_1 \hat{c}_2 \hat{c}_{\frac{9}{2}}^* \hat{c}_7 \hat{c}_{\frac{17}{2}}^* (\hat{d}_{\frac{23}{2}} \hat{c}_{\frac{21}{2}}^*) \hat{c}_{14} \\ &\rightarrow \hat{c}_1 \hat{c}_2 \hat{c}_{\frac{9}{2}}^* \hat{c}_7 \hat{c}_{\frac{17}{2}}^* \hat{c}_{\frac{19}{2}}^* \hat{d}_{\frac{25}{2}} \hat{c}_{14}. \end{aligned}$$

where in each line, we have used parentheses to indicate the pair of symbols affected.

To excite a number of integer valleys simultaneously, we simply add the required excitement to the subscript of each \hat{d}_x in $\hat{\pi}(\hat{h})$, and standardise the resulting word by repeatedly using (44).

We note that, as in the last section, the excitation of an integer valley corresponding to an operator \hat{d}_x in an operator word $\hat{\pi}$ is given by (40), even when the word is non-standard. This is so because the value of the expression (40) is unchanged for operator words obtained from one another through the equivalence (44).

4.3. Bijection relating the \mathcal{P}^p and \mathcal{H}^p paths. The bijection between these two path representations of the $\mathcal{M}(p, 2p + 1)$ models can now be accomplished by mapping from the standard operator word corresponding to one, to an operator word (which may be non-standard) for the other. The appropriate equivalences, either (33) or (44), are then used to obtain the standard operator word, from which the path of the bijective image is readily read.

For odd integers a and b , with $1 \leq a < 2p$ and $3 \leq b < 2p$, let $h \in \mathcal{P}_{a,b}^p$ and let $\hat{h} \in \mathcal{H}_{\hat{a},\hat{b}}^p$ be its image under the bijection of Section 3.1, where $\hat{a} = \frac{1}{2}(a - 1)$ and $\hat{b} = \frac{1}{2}(b - 1)$. We claim that if π is an operator word for h , then $\hat{\pi}$ is an operator word for \hat{h} , where we obtain $\hat{\pi}$ from π by transforming each operator within according to

$$(47) \quad c_x \rightarrow \hat{c}_{x/2}, \quad c_y^* \rightarrow \hat{c}_{y/2}^*, \quad d_x \rightarrow \hat{d}_{x+1/2}.$$

To verify this claim, we show that the paths $h \in \mathcal{P}_{a,b}^p$ and $\hat{h} \in \mathcal{H}_{\hat{a},\hat{b}}^p$, that correspond to the operator words π and $\hat{\pi}$ respectively, are related through the map $h \rightarrow \hat{h}$ defined in Section 3.1.

Let the triple $(h^{\text{cut}}, n, \lambda)$ be that corresponding to h , as defined in Section 3.1. Then h contains n particles and, consequently, π contains n operators d_x . Whether π is standard or non-standard, the excitation λ_i of the particle corresponding to the i th operator d_x , counting from the right, is given by (30). In the case of a standard word π , the standard word $\pi' = \pi(h^{\text{cut}})$ of h^{cut} is obtained from π (as may be seen from Fig. 8) simply by reducing the subscript of each term $c_z^{(*)}$ by $2\#\{d \cdots c_z^{(*)}\}$ (i.e., by twice the number of particles to its left), and dropping all operators d_x . This also holds for non-standard words π , because π' , obtained in this way, is unchanged under the equivalence (33).

We now proceed analogously for the operator word $\hat{\pi}$, determining μ and \hat{h}^{cut} . Since $\hat{\pi}$ has n operators $d_{x'}$, the half-lattice path \hat{h} has n integer valleys. The excitation $\hat{\lambda}_i$ of the i th of these integer valleys, counting from the right, is given by (40), whether $\hat{\pi}$ is standard or non-standard. Since the transformation (47) specifies that $x' = x + 1/2$, we have $\hat{\lambda}_i = \lambda_i$. Thereupon, the value of μ_i , the numbering of the i th integer valley of \hat{h} amongst all its valleys, is given by $\mu_i = \hat{\lambda}_i + \#\{\hat{d} \cdots \hat{d}_{x'}\} + 1 = \lambda_i + n - i + 1$. Thus, λ and μ are related by (17), as required.

In the case of a standard word $\hat{\pi}$, the standard word $\hat{\pi}' = \hat{\pi}(\hat{h}^{\text{cut}})$ of \hat{h}^{cut} is obtained from $\hat{\pi}$ (as may be seen from Fig. 9) simply by reducing the subscript of each term $\hat{c}_z^{(*)}$ by $\#\{\hat{d} \cdots \hat{c}_z^{(*)}\}$ (i.e., by the number of integer valleys to its left), and dropping all operators \hat{d}_x . This also holds for non-standard words $\hat{\pi}$, because $\hat{\pi}'$, obtained in this way, is unchanged under the equivalence (44).

Now, in view of the transformation (47), we see that the subscripts of the terms in π' are precisely twice those in $\hat{\pi}'$. Thus, the particle-deficient path \hat{h}^{cut} is obtained from h^{cut} by shrinking by a factor of 2. Therefore, the combined map $h \rightarrow (h^{\text{cut}}, n, \lambda) \rightarrow (\hat{h}^{\text{cut}}, n, \mu) \rightarrow \hat{h}$ is precisely as specified in Section 3.1. This completes the verification of this operator description of the bijection.

To illustrate the description, consider the path $h \in \mathcal{P}_{1,3}^4$ of Fig. 1. Its standard operator word $\pi(h)$ is given in (28). Using the transformation (47) and the equivalences (44), we

obtain:

$$\begin{aligned}
 c_0 d_2 c_4 c_6 d_{10} c_{13}^* d_{16} d_{19} c_{21}^* &\rightarrow \hat{c}_0 \hat{d}_{\frac{3}{2}} \hat{c}_2 \hat{c}_3 \hat{d}_{\frac{21}{2}} \hat{c}_{13}^* \hat{d}_{\frac{33}{2}} (\hat{d}_{\frac{39}{2}} \hat{c}_{21}^*) \\
 &\rightarrow \hat{c}_0 \hat{d}_{\frac{5}{2}} \hat{c}_2 \hat{c}_3 \hat{d}_{\frac{21}{2}} \hat{c}_{13}^* (\hat{d}_{\frac{33}{2}} \hat{c}_{19}^*) \hat{d}_{\frac{41}{2}} \\
 &\rightarrow \hat{c}_0 \hat{d}_{\frac{5}{2}} \hat{c}_2 \hat{c}_3 (\hat{d}_{\frac{21}{2}} \hat{c}_{13}^*) \hat{c}_{17}^* \hat{d}_{\frac{35}{2}} \hat{d}_{\frac{41}{2}} \\
 &\rightarrow \hat{c}_0 \hat{d}_{\frac{5}{2}} \hat{c}_2 \hat{c}_3 \hat{c}_{11}^* (\hat{d}_{\frac{23}{2}} \hat{c}_{17}^*) \hat{d}_{\frac{35}{2}} \hat{d}_{\frac{41}{2}} \\
 &\rightarrow \hat{c}_0 (\hat{d}_{\frac{5}{2}} \hat{c}_2) \hat{c}_3 \hat{c}_{11}^* \hat{c}_{15}^* \hat{d}_{\frac{25}{2}} \hat{d}_{\frac{35}{2}} \hat{d}_{\frac{41}{2}} \\
 &\rightarrow \hat{c}_0 \hat{c}_1 (\hat{d}_{\frac{7}{2}} \hat{c}_3) \hat{c}_{11}^* \hat{c}_{15}^* \hat{d}_{\frac{25}{2}} \hat{d}_{\frac{35}{2}} \hat{d}_{\frac{41}{2}} \\
 &\rightarrow \hat{c}_0 \hat{c}_1 \hat{c}_2 (\hat{d}_{\frac{9}{2}} \hat{c}_{11}^*) \hat{c}_{15}^* \hat{d}_{\frac{25}{2}} \hat{d}_{\frac{35}{2}} \hat{d}_{\frac{41}{2}} \\
 &\rightarrow \hat{c}_0 \hat{c}_1 \hat{c}_2 \hat{c}_{\frac{9}{2}}^* \hat{d}_{\frac{11}{2}} \hat{c}_{15}^* \hat{d}_{\frac{25}{2}} \hat{d}_{\frac{35}{2}} \hat{d}_{\frac{41}{2}}.
 \end{aligned}$$

Here, we have used parentheses to indicate the operators reordered by means of (44). We recognize the final word here to be (38), the standard operator word corresponding to the path of Fig. 2.

To illustrate the inverse mapping, begin with the standard operator word (38). Applying the reverse of the transformations (47), and standardising the result using (33) produces

$$\begin{aligned}
 \hat{c}_0 \hat{c}_1 \hat{c}_2 \hat{c}_{\frac{9}{2}}^* \hat{d}_{\frac{11}{2}} \hat{c}_{15}^* \hat{d}_{\frac{25}{2}} \hat{d}_{\frac{35}{2}} \hat{d}_{\frac{41}{2}} &\rightarrow c_0 (c_2 c_4 c_9^* d_5) c_{15}^* d_{12} d_{17} d_{20} \\
 &\rightarrow c_0 d_2 c_4 c_6 (c_{11}^* c_{15}^* d_{12}) d_{17} d_{20} \\
 &\rightarrow c_0 d_2 c_4 c_6 d_{10} c_{13}^* (c_{17}^* d_{17}) d_{20} \\
 &\rightarrow c_0 d_2 c_4 c_6 d_{10} c_{13}^* d_{16} (c_{19}^* d_{20}) \\
 &\rightarrow c_0 d_2 d_4 c_6 d_{10} c_{13}^* d_{16} d_{19} c_{21}^*,
 \end{aligned}$$

thus recovering the operator sequence (28) of our original path, Fig. 1. Here, in each line, we have used parentheses to indicate a number of applications of (33) which are applied successively within the included subword to shift the operator d completely to the left.

5. OUTLOOK

There is a well-known duality between the characters of the $\mathcal{M}(p, p')$ and $\mathcal{M}(p' - p, p')$ models [3]. In terms of RSOS paths, this duality involves interchanging the role of the light and dark bands [7]. This hints at a description of the $\mathcal{M}(p + 1, 2p + 1)$ states in terms of some sort of dual half-lattice paths. It turns out that such a description does exist. Roughly, these are half-lattice paths with half-integer extremity conditions (instead of integer ones) and with peaks at half-integer heights.

To be more precise, let us denote the set of new paths by $\tilde{\mathcal{H}}_{\tilde{a}, \tilde{b}}^p$, where $\tilde{a}, \tilde{b} \in \mathbb{Z} + \frac{1}{2}$. This set is defined to contain all half-lattice paths \hat{h} that are $(0, p - 1/2)$ -restricted, \tilde{b} -tailed, with $\hat{h}_0 = \tilde{a}$, and the additional restriction that if $\hat{h}_x = \hat{h}_{x+1} \in \mathbb{Z} + \frac{1}{2}$, then $\hat{h}_{x+1/2} = \hat{h}_x - 1/2$. This additional restriction forces the peaks to occur at non-integer heights (however, the half-integer initial point ensures that all peaks occur at integer x -positions). These paths are weighted similarly to their dual versions, using (7) and (8). As announced, these new paths describe the states in the (r, s) irreducible module of $\mathcal{M}(p + 1, 2p + 1)$ where

$$(48) \quad r = \tilde{a} + \frac{1}{2} \quad \text{and} \quad s = 2\tilde{b}.$$

Note that, in comparison with the \mathcal{H}^p paths (see (13)), the roles of \tilde{a} and \tilde{b} have interchanged in that, here, \tilde{a} and \tilde{b} are related to r and s respectively. Note also that the vertical range is larger for paths in $\tilde{\mathcal{H}}_{\tilde{a}, \tilde{b}}^p$ than for those in $\mathcal{H}_{\tilde{a}, \tilde{b}}^p$, being $p - 1/2$ and $p - 1$ respectively. However, as previously mentioned, in the latter case, the maximal height could be augmented to $p - 1/2$ without affecting the set of paths since the constraints on the integrality of the peaks' heights

prevents the extra portion from being reached. Therefore, both the \mathcal{H}^p and the $\tilde{\mathcal{H}}^p$ paths can be defined in the same strip, enhancing their duality relationship.

Following the analysis of [15], this path representation leads to new expressions for the $\mathcal{M}(p + 1, 2p + 1)$ fermionic characters and with a clear particle content. This will be detailed elsewhere.

Finally, aspects of the present bijection can be turned into a well-controlled exploratory tool for an alternative path description of the $\mathcal{M}(p, fp + 1)$ models on a $(1/f)$ -lattice, with special restrictions on the positions of the peaks and valleys. As already stressed, this is interesting in that it could lead to novel fermionic forms. Such a study is left to a future work.

Acknowledgments. *OBf acknowledges a NSERC student fellowship and thanks the Institut Henri Poincaré and the Centre Émile Borel for its hospitality in the course of the thematic semester Statistical physics, combinatorics and probability: from discrete to continuous models, during which part of this work was done. This work was supported by NSERC.*

REFERENCES

- [1] G.E. Andrews, R.J. Baxter and P.J. Forrester, *Eight-vertex SOS model and generalized Rogers-Ramanujan-type identities*, J. Stat. Phys. **35** (1984) 193–266.
- [2] R.J. Baxter, *Exactly Solved Models in Statistical Mechanics*, 1982 (Academic Press, London); 2007 (Dover, New York).
- [3] A. Berkovich and B.M. McCoy, *Continued fractions and fermionic representations for characters of $\mathcal{M}(p, p')$ minimal models*, Lett. Math. Phys. **37** (1996) 49–66.
- [4] J.M. Camino, A.V. Ramallo and J.M. Sanchez de Santos, *Graded parafermions*, Nucl. Phys. **B530** (1998) 715–741.
- [5] E. Date, M. Jimbo, A. Kuniba, T. Miwa and M. Okado, *Exactly solvable SOS models: local height probabilities and theta function identities*, Nucl. Phys. **B290** (1987) 231–273.
- [6] P. Di Francesco, P. Mathieu and D. Sénéchal, *Conformal Field Theory*, 1997 (Springer-Verlag, New York).
- [7] O. Foda, K.S.M. Lee, Y. Pugai and T.A. Welsh, *Path generating transforms*, Contemp. Math. **254** (2000) 157–186.
- [8] O. Foda and Y.-H. Quano, *Virasoro character identities from the Andrews-Bailey construction*, Int. J. Mod. Phys. **A12** (1997) 1651–1675.
- [9] O. Foda and T.A. Welsh, *Melzer’s identities revisited*, Contemp. Math. **248** (1999) 207–234.
- [10] O. Foda and T.A. Welsh, *On the combinatorics of Forrester-Baxter models*, in proceedings of “Physical Combinatorics”, Kyoto 1999, eds. M. Kashiwara and T. Miwa, *Prog. Math.* **191**, 2000 (Birkhäuser, Boston), pp. 49–103.
- [11] P.J. Forrester and R.J. Baxter, *Further exact solutions of the eight-vertex SOS model and generalizations of the Rogers-Ramanujan identities*, J. Stat. Phys. **38** (1985) 435–472.
- [12] P. Jacob and P. Mathieu, *Graded parafermions: standard and quasi-particle bases*, Nucl. Phys. **B630** (2002) 433–452.
- [13] P. Jacob and P. Mathieu, *Paths for $\bar{\mathcal{Z}}_k$ parafermionic models*, Lett. Math. Phys. **81** (2007) 211–226.
- [14] P. Jacob and P. Mathieu, *Nonlocal operator basis from the path representation of the $\mathcal{M}(k + 1, k + 2)$ and the $\mathcal{M}(k + 1, 2k + 3)$ minimal models*, J. Phys. A **41** (2008) 385201–21.
- [15] P. Jacob and P. Mathieu, *A new path description for the $\mathcal{M}(k + 1, 2k + 3)$ models and the dual $\bar{\mathcal{Z}}_k$ graded parafermions*, J. Stat. Mech. (2007) P11005 (43 pp.).
- [16] P. Jacob and P. Mathieu, *Particles in RSOS paths*, J. Phys. A **42** (2009) 122001–16.
- [17] R. Kedem, T.R. Klassen, B.M. McCoy and E. Melzer, *Fermionic sum representations for conformal field theory characters*, Phys. Lett. B **307** (1993) 68–76.
- [18] P. Mathieu, *Paths and partitions: combinatorial descriptions of the parafermionic states*, J. Math. Phys. **50** (2009) 095210 (43 pp.).
- [19] E. Melzer, *Fermionic character sums and the corner transfer matrix*, Int. J. Mod. Phys. **A9** (1994) 1115–1136.
- [20] A. Rocha-Caridi, *Vacuum vector representations of the Virasoro algebra*, in proceedings of “Vertex Operators in Mathematics and Physics”, eds. J. Lepowsky, S. Mandelstam and I.M. Singer, 1985 (Springer-Verlag, New York), pp. 451–473.
- [21] S.O. Warnaar, *Fermionic solution of the Andrews-Baxter-Forrester model. I. Unification of CTM and TBA methods*, J. Stat. Phys. **82** (1996) 657–685; *Fermionic solution of the Andrews-Baxter-Forrester model. II. Proof of Melzer’s polynomial identities*, J. Stat. Phys. **84** (1996), 49–83.

- [22] T.A. Welsh, *Paths, Virasoro characters and fermionic expressions*, in proceedings of “Symmetry and Structural Properties of Condensed Matter”, Myczkowce, Poland, September 2005, J. Phys.: Conf. Ser. **30** (2006) 119–132.
- [23] T.A. Welsh, *Fermionic expressions for minimal model Virasoro characters*, Mem. Amer. Math. Soc. **175** (no. 827) 2005.

DÉPARTEMENT DE PHYSIQUE, DE GÉNIE PHYSIQUE ET D'OPTIQUE, UNIVERSITÉ LAVAL, QUÉBEC, CANADA, G1K 7P4.

E-mail address: `olivier.b-fourrier.1@ulaval.ca`

DÉPARTEMENT DE PHYSIQUE, DE GÉNIE PHYSIQUE ET D'OPTIQUE, UNIVERSITÉ LAVAL, QUÉBEC, CANADA, G1K 7P4.

E-mail address: `pmathieu@phy.ulaval.ca`

DEPARTMENT OF PHYSICS, UNIVERSITY OF TORONTO, ONTARIO, CANADA, M5S 1A7.

E-mail address: `trevor.welsh@utoronto.ca`